2005

Involvement of human MOF in ATM function

Arun Gupta
Washington University School of Medicine in St. Louis

Girdhar G. Sharma
Washington University School of Medicine in St. Louis

Charles S. H. Young
Columbia University

Manjula Agarwal
Washington University School of Medicine in St. Louis

Edwin R. Smith
Emory University

See next page for additional authors

Involvement of Human MOF in ATM Function

Arun Gupta, Girdhar G. Sharma, Charles S. H. Young, Manjula Agarwal, Edwin R. Smith, Tanya T. Paull, John C. Lucchesi, Kum Kum Khanna, Thomas Ludwig and Tej K. Pandita

***Mol. Cell. Biol.* 2005, 25(12):5292. DOI: 10.1128/MCB.25.12.5292-5305.2005.**

MOLECULAR AND CELLULAR BIOLOGY, June 2005, p. 5292–5305 Vol. 25, No. 12
0270-7306/05/$08.00+0 doi:10.1128/MCB.25.12.5292–5305.2005

Involvement of Human MOF in ATM Function

Arun Gupta,[1] Girdhar G. Sharma,[1] Charles S. H. Young,[2] Manjula Agarwal,[1] Edwin R. Smith,[3]† Tanya T. Paull,[4] John C. Lucchesi,[3] Kum Kum Khanna,[5] Thomas Ludwig,[2] and Tej K. Pandita[1]*

Department of Radiation Oncology, Washington University School of Medicine, St. Louis, Missouri 63108[1]; College of Physicians and Surgeons, Columbia University, New York, New York 10032[2]; Department of Biology, Emory University, Atlanta, Georgia 30322[3]; University of Texas at Austin, Austin, Texas 78712[4]; and Queensland Institute of Medical Research, Brisbane, Queensland 4029, Australia[5]

Received 22 October 2004/Returned for modification 13 December 2004/Accepted 21 March 2005

We have determined that *hMOF*, the human ortholog of the *Drosophila MOF* gene (males absent on the first), encoding a protein with histone acetyltransferase activity, interacts with the ATM (ataxia-telangiectasia-mutated) protein. Cellular exposure to ionizing radiation (IR) enhances hMOF-dependent acetylation of its target substrate, lysine 16 (K16) of histone H4 independently of ATM function. Blocking the IR-induced increase in acetylation of histone H4 at K16, either by the expression of a dominant negative mutant ΔhMOF or by RNA interference-mediated hMOF knockdown, resulted in decreased ATM autophosphorylation, ATM kinase activity, and the phosphorylation of downstream effectors of ATM and DNA repair while increasing cell killing. In addition, decreased hMOF activity was associated with loss of the cell cycle checkpoint response to DNA double-strand breaks. The overexpression of wild-type hMOF yielded the opposite results, i.e., a modest increase in cell survival and enhanced DNA repair after IR exposure. These results suggest that hMOF influences the function of ATM.

In eukaryotic cells, DNA damage activates signal transduction pathways that rapidly affect downstream processes such as gene transcription, cell cycle progression, and DNA replication (13, 25). All of these processes involve alterations in chromatin structure. Posttranslational covalent modifications of histones have emerged as key regulatory events in DNA damage response. A widespread modification is acetylation catalyzed by histone acetyltransferases and reversed by deacetylases (3, 13, 50). Reversible acetylation of four lysines (K) at positions 5, 8, 12, and 16 in the amino-terminal tail of histone H4 occurs in vivo in all eukaryotes (3). The hyperacetylation of histone H4 could lead to the unfolding of the nucleosomal fiber (50), and the acetylation of histone H4 at K16 occurs on the hyperactive male X chromosome of *Drosophila* polytene chromosomes (51). Ikura et al. (19) noted that Tip60 (Tat-interacting protein), which acetylates histones H2A, H3, and H4, plays a role in DNA repair. More recently, Kusch et al. (28) demonstrated that the *Drosophila* Tip60 acetylates nucleosomal phospho-H2Av and exchanges it with an unmodified H2Av. Bird et al. (5) reported that the acetylation of histone H4 by Esa1 (essential SAS2-related acetyltransferase) is required for DNA repair in yeast and suggested that a similar modification may function in mammalian cells.

ATM (ataxia-telangiectasia-mutated protein) is crucial for the initiation of signaling pathways in mammalian cells following exposure to ionizing radiation (IR) and other DNA-damaging agents (36, 46), and cells deficient in ATM function also have defective telomere chromatin (47). Bakkenist and Kastan (4) have suggested that chromatin structural perturbations induced by DNA double-strand breaks (DSBs) serve as a trigger for ATM activation. Recent studies indicate that the MRN (Mre11, Rad50, and Nbs1) complex as well as TRF2 either influences activation of ATM (9, 29, 52) or serves as a modulator/amplifier of ATM activity (17, 23). Our studies on DNA and chromosome damage after treatment with IR suggested that cells deficient in ATM function were less efficient in blocking the conversion of DNA damage into chromosome damage (33, 38, 40), possibly indicating an inherent chromatin alteration (16, 39). ATM has been reported to regulate the function of some histone-modifying factors (22, 27). In this report, we have identified hMOF as an ATM-interacting protein and have provided evidence that functional hMOF participates in the activation of ATM in response to DNA damage. hMOF is the human ortholog of *Drosophila* MOF, a histone acetyltransferase that modifies the X-chromosome chromatin in males in order to achieve dosage compensation (15).

MATERIALS AND METHODS

Yeast two-hybrid screen. The procedure for the construction of hMOF or its fragments is the same as that used for ATM and TRF1 and has been described previously (30, 33, 45, 48). The yeast two-hybrid screen was performed by the transformation of yeast strain Y153 containing plasmid pHM677 (Y153/pHM677) with a cDNA library from human embryonic cells (Clontech). Primary transformants were analyzed for interaction with ATM by selection for histidine prototrophy on dropout plates supplemented with 20 mM 3-aminotriazole and for the expression of β-galactosidase (β-gal) as determined by filter lift tests. Plasmids encoding putative binding partners of ATM were then isolated from double-positive yeast clones and retransformed into Y153/pHM677 in order to confirm the interactions. Positive clones after retransformation were subjected to automated sequencing and homology searches using a BLAST (tBLASTn) search of the GenBank human database. Several putative cellular binding partners of ATM were identified. Most of them were isolated in several copies. To quantify the interaction between ATM and hMOF, interactions between hMOF (wild type and mutated) and ATM fragments in liquid β-gal were assayed (Fig. 1) according to the previously described procedure (12, 30).

* Corresponding author. Mailing address: Department of Radiation Oncology, Washington University School of Medicine, 4511 Forest Park, St. Louis, MO 63108. Phone: (314) 747-5461. Fax: (314) 362-9790. E-mail: pandita@wustl.edu.

† Present address: Laboratory of Chromatin Biology, Rockefeller University, 1230 York Avenue, New York, NY 10021.

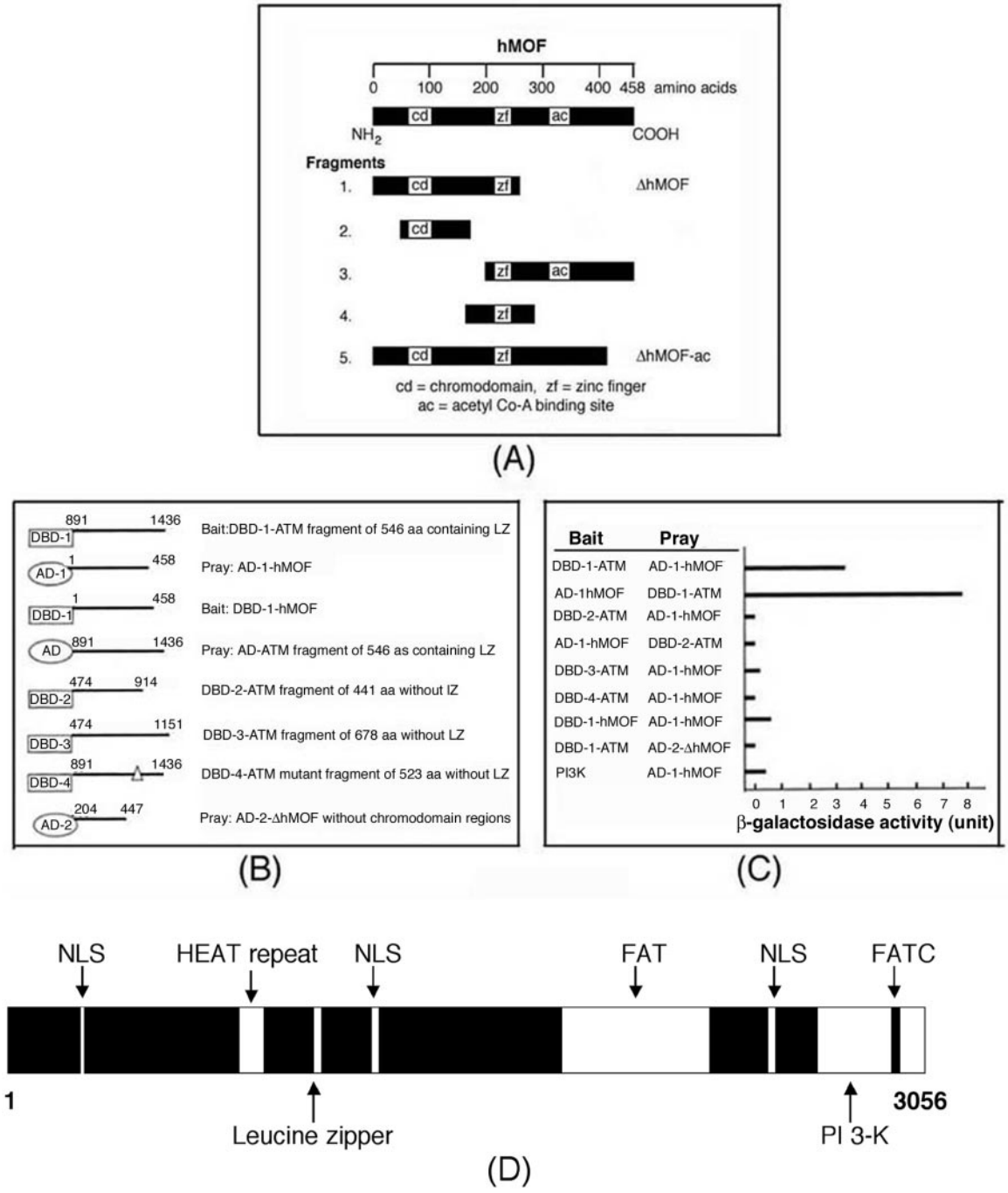

FIG. 1. Yeast two-hybrid-binding assays. (A) hMOF cDNA fragments generated by PCR. (B) The Gal4 DNA-binding domain (DBD) was fused to bait (hMOF, hMOF fragments, or ATM fragments), and the activation domain (AD) of Gal4 was fused to prey (ATM fragments, hMOF, or hMOF fragments). DNA-binding domain 4, which lacks amino acids 1217 to 1239, was generated as described previously (10). (C) Plasmids in pairs were introduced into *Saccharomyces cerevisiae* HF7c cells, and β-gal activity was quantified by using an *O*-nitrophenyl β-D-galactoside assay. (D) Schematic representation of the domains of the ATM protein. NLS, nuclear localization signal.

Cell culture and derivation of cell lines. AT221JE-TpEBS7 (A-T [ataxia-telangiectasia] fibroblast with empty vector only), AT221JE-TpEBS7-YZ5 (A-T fibroblast complemented with ATM cDNA), GM5849, and 293 cells were maintained and transfected with plasmids as described previously (45). Complementary DNAs encoding wild or mutant hMOF (ΔhMOF) were cloned into the mammalian expression vector pIND(SP1)/Neo (Invitrogen, Carlsbad, CA) as described previously (18, 45). Mutant forms of hMOF were created by using a PCR approach with appropriate primer pair combinations. ATMΔLZ was generated as described previously (10). The wild or mutant forms tagged to GFP, HA, or Flag were cloned into the pIND(SP1)/Neo vector. The final constructs were verified by DNA sequencing. An adenoviral construct expressing hMOF (Ad.hMOF) was constructed as described previously (44). hMOF small interfering RNA (siRNA) and control Luc siRNA were obtained from Dharmacone Research (Lafayette, CO). We also used the hMOF siRNA vector pRNA-U6.1/Neo (GeneScript).

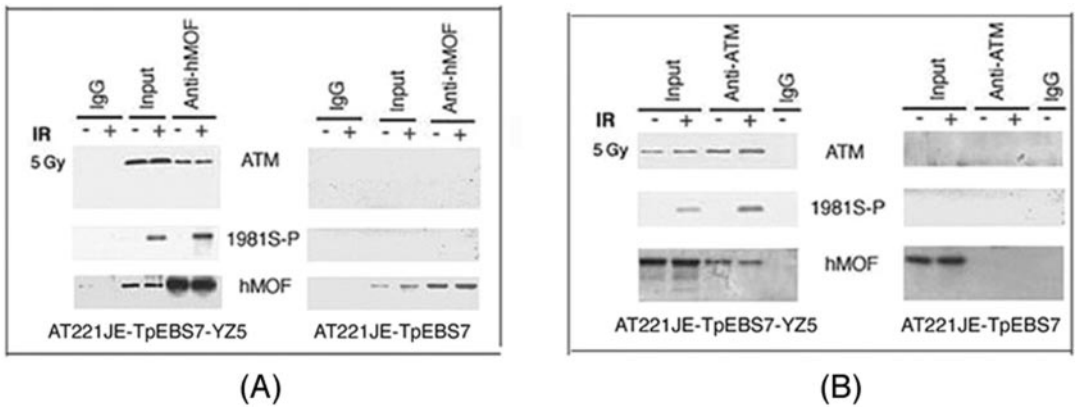

FIG. 2. hMOF and ATM interaction. The specific interaction between ATM and hMOF is shown as determined by coIP experiments. Cells were harvested 1 h postirradiation. IP or immunoblotting was done with the hMOF or ATM- or species-matched immunoglobulin G (IgG) control antibodies. Input represents 50% of the total protein used in IPs. Cell lysates were made from AT221JE-TpEBS7-YZ5 (A-T fibroblast with ATM cDNA complementation) and AT22IJE-TpEBS7 (A-T fibroblasts with empty vector only) cells. (A) IP was performed with anti-hMOF antibodies. Coprecipitated ATM was detected in Western blot analysis with the anti-ATM antibody only in AT22IJE-TpEBS7-YZ5 cells. IR-induced ATM phosphorylation was detected by anti-p-Ser-1981 ATM antibody. (B) Reciprocal IP with ATM to detect hMOF in the ATM complex. Coprecipitated hMOF was detected only in AT22IJE-TpEBS7-YZ5 using the anti-ATM antibody.

Western analysis, immunoprecipitation, HAT, and ATM kinase assays. Cell lysates were prepared according to the previously described procedure (41). Polyclonal hMOF antibody raised in rabbit has been described previously (34). Immunoblotting and detections for hMOF and ATM were done according to a previously described procedure (41, 45). For immunoprecipitation (IP), cells were broken in lysis buffer as described previously (41). Lysates were precleaned with purified immunoglobulin G and protein A/G beads. Proteins were immunoprecipitated with specific antibodies, and immunoprecipitants were washed with lysis buffer as described previously (41). An ATM kinase assay was performed as described previously (41). A histone acetyltransferase (HAT) assay was performed according to the manufacturer's instructions (Upstate Biotechnology).

Assay for ionizing radiation sensitivity. Cells were plated in 35-mm dishes. The cell count was determined using a Coulter counter. Cells were plated as single cells into 60-mm dishes in 5 ml of media, incubated for 6 h, and subsequently exposed to IR. The actual amounts of cells per dish were chosen to ensure that about 50 colonies would survive a particular radiation dose treatment. Cells were exposed to IR in the dose range of 0 to 8 Gy at room temperature. Cells were incubated for 12 or more days and were fixed in methanol: acetic acid (3:1) prior to staining with crystal violet. Only colonies containing >50 cells were counted.

Metaphase chromosome spreads were prepared by procedures described previously (35). Giemsa-stained chromosomes of metaphase spreads were analyzed for chromosome end-to-end associations. G_1 phase-specific chromosomal aberrations were assessed as described previously (37). Briefly, cells in plateau phase were irradiated with 3 Gy, allowed to incubate for 24 h, and subcultured, and metaphases were collected. Chromosome spreads were prepared by the procedure described previously (35). The categories of G_1-type asymmetrical chromosome aberrations scored included dicentrics, centric rings, interstitial deletions/acentric rings, and terminal deletions.

S-phase-specific chromosomal aberrations were analyzed at metaphase. Exponentially growing cells were treated with 2 Gy of gamma radiation, and mitotic cells were collected 3 to 6 h after irradiation. Both chromosome- as well as chromatid-type aberrations were scored. For G_2 phase-specific chromosomal aberrations, cells in exponential phase were irradiated with 1 Gy, and metaphases were collected at 45 and 90 min following irradiation and examined for chromatid breaks and gaps per metaphase as described previously (33).

Neutral filter elution. The level of DNA DSBs in cells was estimated as described previously (40). Cells were labeled for a period of one-and-one-half doublings and then were washed free of radioactive medium and reincubated in nonradioactive medium for an additional 3 h prior to the experiment. Cells were exposed to IR and incubated at 37°C for different times postirradiation. Cells were layered onto polycarbonated filters, lysed, and eluted under neutral conditions (pH 9.6) as described previously (40). Relative elution (RE) was calculated as $RE = -\log(FI/Fc)$, where FI and Fc are the fractions of DNA left on the filter for the irradiated (I) and unirradiated (c) cells when 75% of the internal standard DNA is left on the filter.

RESULTS

Using a modified yeast two-hybrid screen (12, 30) described in Materials and Methods, several putative cellular binding partners of ATM were isolated, including two encoded by cDNAs identified from DNA sequence analysis as human orthologs of *Drosophila MOF* (15). The longer of the two cDNAs was 1.8 kb and encoded a 458-amino-acid protein with a mass of 52.4 kDa containing a chromodomain region, a zinc finger, and an acetyl coenzyme A (acetyl-CoA)-binding site with HAT activity directed toward histones H3, H2A, and H4 (34).

The interaction between hMOF and ATM was examined by liquid β-gal assays (Fig. 1). Full-length hMOF and ATM fragments containing leucine zippers (LZ) exhibited 3.4- to 7.8-fold higher β-gal activities than that observed for the empty vector control. Minimum interactions were found between ATM fragments containing the PI3-kinase domain and hMOF or between hMOF proteins. Deletion of the region containing the LZ domain of the ATM fragment or deletion of the region containing the chromodomain of hMOF resulted in a loss of interaction, establishing that the association of the two proteins occurs via the interaction of these regions containing the domains (Fig. 1).

To confirm that the interactions between ATM and hMOF occurred in mammalian cells, we performed coimmunoprecipitation (coIP) experiments. Anti-ATM antibody immunoprecipitated endogenous hMOF only from cells expressing functional ATM, and the association between the two proteins did not change after exposure to IR (Fig. 2A). The reciprocal immunoprecipitation yielded the same results (Fig. 2B). The association of hMOF and ATM was also confirmed in nonisogenic cells with respect to ATM function (data not shown).

The region of ATM responsible for the interactions with hMOF was determined in vitro by incubating glutathione-*S*-

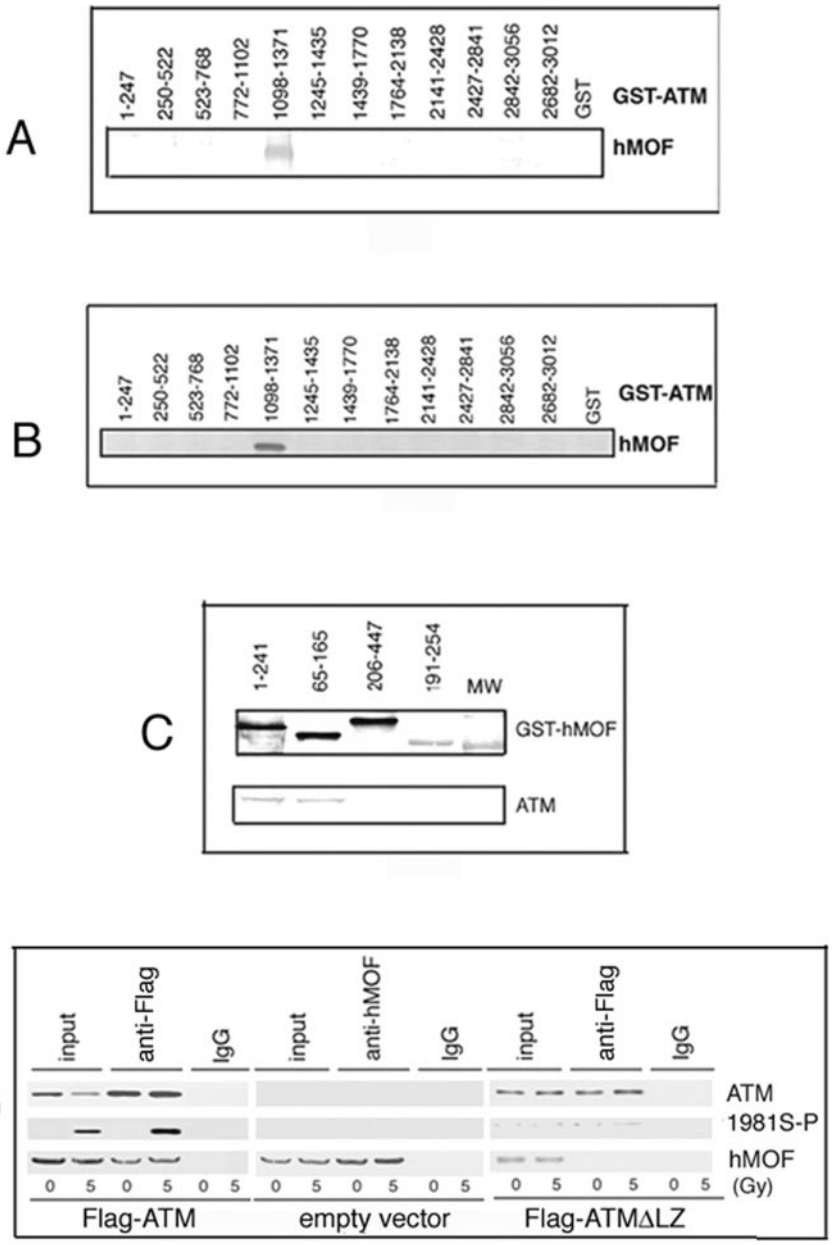

FIG. 3. In vitro mapping the region of ATM that interacts with hMOF. Binding and detection of in vitro-translated hMOF (A) or 293 cell extracts (B) with a series of GST-ATM proteins was performed according to previously described procedures (26). (C) Mapping the region of hMOF that interacts with ATM. Bacterially expressed GST-hMOF fusion proteins were incubated with 293 cell extracts, and bound protein was analyzed by immunoblotting with ATM antibody. (D) The LZ region of ATM is essential for interaction with hMOF and in vivo IR-induced Ser-1981 ATM phosphorylation. AT22IJE (deficient in ATM) cells were transfected with either Flag-tagged ATMΔLZ or Flag-tagged ATM and treated with 5 Gy. ATMΔLZ did not coimmunoprecipitate with hMOF, nor did ATMΔLZ autophosphorylate upon IR.

transferase (GST)-ATM proteins with in vitro transcribed and translated ^{35}S-labeled hMOF protein as described previously (26). hMOF interacted only with a GST-ATM fragment (amino acids 1098 to 1371) containing the LZ region (Fig. 3A). To confirm the interaction of endogenous hMOF with the GST-ATM fusion protein, extracts from 293 cells were mixed with beads containing GST or GST-ATM proteins. The bound protein was analyzed by immunoblotting with hMOF antibody. The results of these experiments clearly delineate the LZ region of ATM as the domain interacting with hMOF (Fig. 3B). To map the hMOF domain interacting with ATM, four GST-hMOF deletion constructs, collectively spanning the entire open reading frame of hMOF, were generated by reverse transcriptase PCR and expressed in bacterial cells. Cell extracts of 293 cells were mixed with agarose beads coated with the GST-hMOF fusion proteins. The GST pull-down results identified the chromodomain region of hMOF as the site interacting with ATM (Fig. 3C). Subsequently, the physiological relevance of the interaction of the LZ region of ATM with hMOF was established by coexpressing Flag-tagged ATMΔLZ (ATM with

a deletion of the LZ region) (10) and hMOF in ATM-deficient (AT221JE) cells and then examined for IR-induced ATM autophosphorylation. Deletion of the LZ region in ATM resulted in a loss of interaction with hMOF and also IR-induced ATM autophosphorylation (Fig. 3D). Such results are consistent with the fact that ATMΔLZ retains kinase activity in vitro; however, it is unable to phosphorylate its substrates in vivo (10).

IR enhances hMOF-mediated acetylation of histone H4 at K16. To test whether IR exposure alters hMOF levels or activity in the presence or absence of functional ATM, cells in exponential phase were irradiated, and hMOF protein levels were determined at increasing intervals postirradiation. Exposure to IR altered neither hMOF protein levels (Fig. 4A) nor its H4 peptide acetylation activity (Fig. 4B), irrespective of whether cells expressed ATM or not. Like its ortholog in *Drosophila* (1, 49) and in contrast to yeast Esa1p or mammalian Tip60, hMOF acetylates histone H4 uniquely at lysine 16 (E. R. Smith and J. C. Lucchesi, unpublished observation). Using an antibody specific for human H4 acetylated at K16, we detected an increase in the acetylation of histone H4 following IR exposure without any detectable change in overall histone H4 levels (Fig. 5B). Cells with (293) and without (GM 5849) functional ATM did not show any difference in histone acetylation, suggesting that K16 acetylation of histone H4 by hMOF is independent of ATM function (Fig. 5B). To determine whether the increased K16 acetylation of histone H4 after IR exposure was due specifically to hMOF activity, cells either expressing mutant hMOF (ΔMOF; fragment 1 of Fig. 1A) or with hMOF knockdown were analyzed by Western blotting for IR-induced acetylation of histone H4 at K16. In comparison to the levels in the control, only cells expressing ΔhMOF (Fig. 1A) or cells with hMOF knockdown (Fig. 5C) had decreased acetylation of histone H4 at K16 after IR exposure (Fig. 5B, D), irrespective of the presence of ATM; cells overexpressing full-length hMOF (Fig. 5A) had higher levels of IR-induced K16 acetylation of histone H4 than control cells did (Fig. 5B). These results suggest that IR exposure enhances hMOF-dependent acetylation of histone H4 at K16 independently of ATM function.

hMOF inactivation abrogates ATM activation. We tested whether the inactivation of hMOF has any influence on IR-induced ATM activation. The expression of ΔhMOF abrogated ATM autophosphorylation in irradiated cells (Fig. 6A), whereas the expression of hMOF fragments 2 to 4 had little effect on ATM autophosphorylation (data not shown). To determine whether the hMOF association influences ATM autophosphorylation, cells expressing HA-tagged wild-type hMOF and ΔhMOF were irradiated and examined for ATM Ser1981 phosphorylation (Fig. 6B). Interestingly, ATM complexed with full-length hMOF displayed IR-induced ATM phosphorylation (Fig. 6Ba), whereas no such phosphorylation was observed in ATM associated with the ΔhMOF deletion mutant (Fig. 6Bb). The influence of hMOF on IR-induced ATM autophosphorylation is consistent with the influence of hMOF on ATM monomerization (Fig. 6C). Furthermore, cells expressing ΔhMOF or cells with hMOF knockdown also had greatly reduced IR-induced ATM kinase activity, as determined by an in vitro kinase assay (Fig. 6D) (41).

To determine whether an increase in the acetylation of histone H4 at K16 alone could influence ATM activation, cells were treated with either 100 nM of the deacetylase inhibitor trichostatin A (TSA) or 5 mM of sodium butyrate (NaB) for 4 h. TSA and NaB enhanced the level of acetylated histone H4 at K16, with a slight effect, in the case of TSA, on ATM autophosphorylation but not on ATM kinase activity (Fig. 6E). The high levels of IR-induced autophosphorylation of ATM and ATM kinase activity were unaffected by the TSA-enriched acetylation of histone H4 at K16. These results suggest that IR-induced acetylation of histone H4 at K16 by hMOF along with DNA breaks induced by IR exposure may induce changes in the chromatin structure and that such chromatin changes

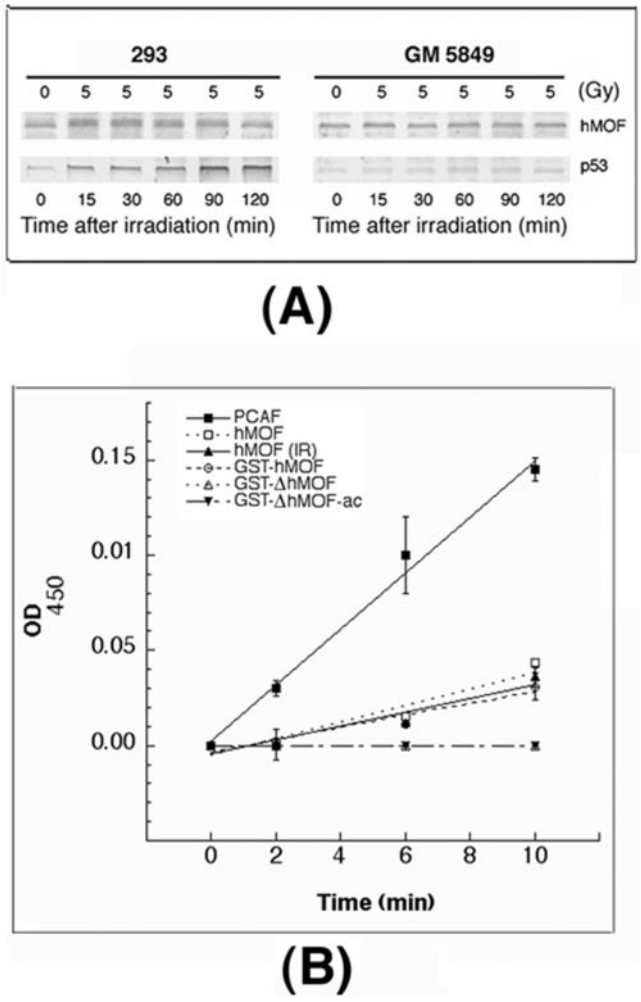

FIG. 4. Effect of IR on hMOF levels and its activity. (A) Cells with ATM (293) and without ATM (GM 5849) were exposed to 5 Gy and examined for hMOF and p53 levels at various times postirradiation. Note there is no change in hMOF levels; however, p53 levels increased in 293 cells but not in GM 5849 cells postirradiation. (B) HAT assay for hMOF. Purified wild-type recombinant GST-hMOF, purified recombinant GST-ΔhMOF, purified recombinant GST-ΔhMOF-ac, and immunoprecipitated hMOF from control and irradiated 293 cells (25 ng per assay) were added to a HAT reaction mixture containing acetyl coenzyme A (HAT assay kit; Upstate Biotechnology). Biotinylated histone H4 peptides were acetylated by wild-type hMOF but not by ΔhMOF or ΔhMOF-ac. Recombinant PCAF (25 ng per assay) was used as a positive control for the HAT assay.

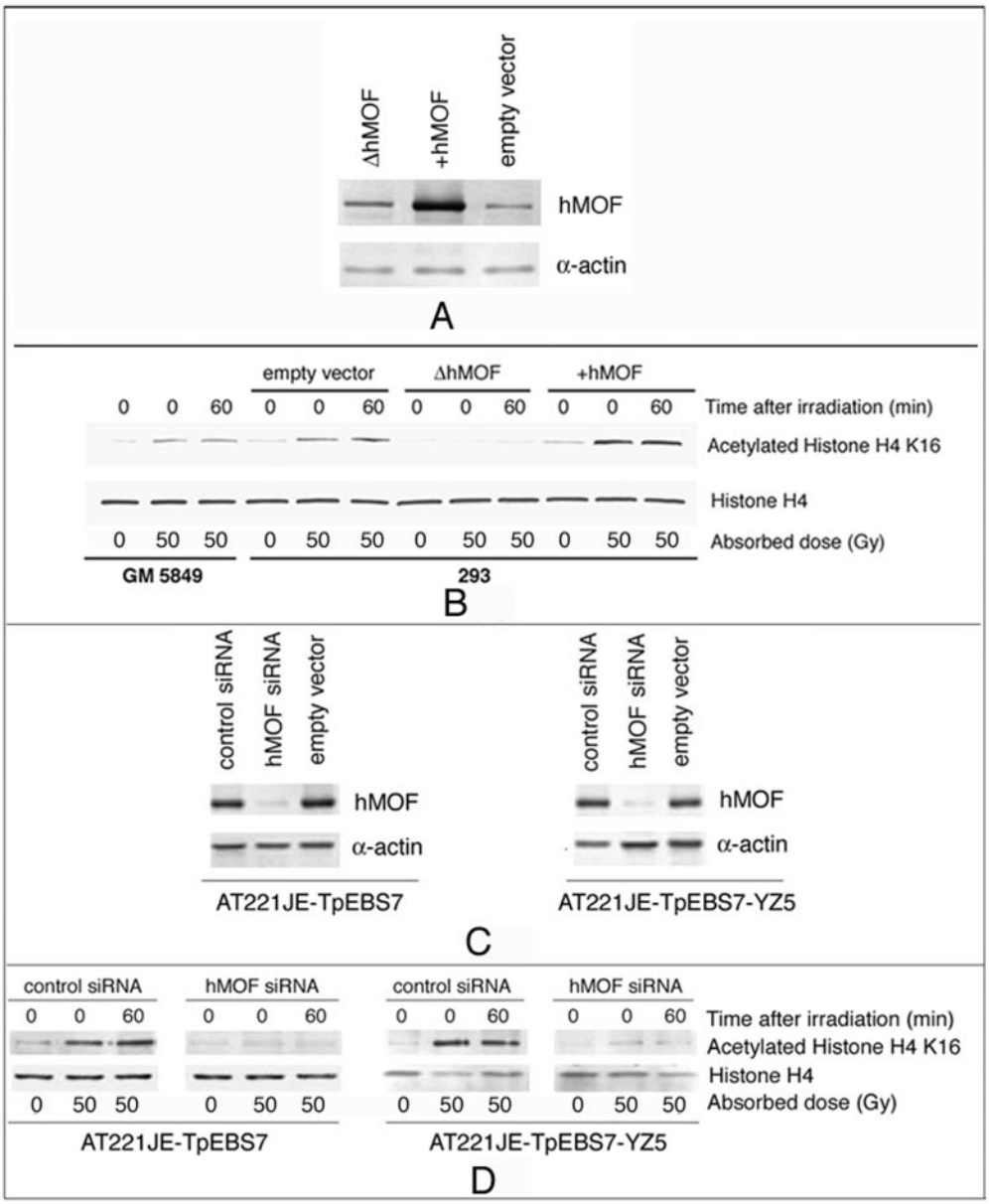

FIG. 5. Effect of IR exposure on the acetylation of histone H4 at K16. (A) Ad.hMOF was constructed as described previously (44). hMOF levels were detected by Western blotting using hMOF-specific antibody. Higher levels of hMOF were observed in cells overexpressing hMOF (+hMOF). (B) Analysis of extracts from GM5849, 293 cells infected with an empty adenovirus vector, 293 cells with expression of ΔhMOF-ac, and 293 cells infected with Ad.hMOF for the levels of histone H4 and acetylated histone H4 K16. Histone H4 levels do not change in any cell type after IR. However, cells expressing ΔhMOF have a minimum increase in the level of acetylated histone H4 K16, whereas cells overexpressing hMOF have higher levels of acetylated histone H4 K16 after IR treatment, demonstrating that hMOF does acetylate histone H4 at K16. (C) siRNA-mediated reduction of hMOF protein in isogenic cells with respect to ATM function. (D) Reduced hMOF expression results in the loss of IR-induced acetylation of histone H4 at K16 in cells with and without ATM.

may be transduced by hMOF to ATM for its activation. We also tested whether hMOF could influence ATM activation in a nonchromatin context. To address this issue, we exploited the in vitro system for MRN-dependent substrate phosphorylation by ATM as described previously (29). Our analysis revealed that hMOF does not alter ATM function in vitro (Fig. 7), supporting the argument that hMOF may act as a transducer of chromatin structural alterations to ATM after DNA damage.

hMOF influences ATM-mediated phosphorylation of downstream effectors. In mammalian cells, in response to DNA damage, ATM phosphorylates various proteins that control G_1, S, and G_2 cell cycle arrest (13, 36, 46). We examined whether the inactivation of hMOF influences ATM-mediated IR-induced phosphorylation on Chk2 in 293 cells. ATM phosphorylates Chk2 on Thr-68 in response to DNA damage (31), which activates Chk2 to phosphorylate substrates including p53 and Cdc25 (32). Cells (293) expressing ΔhMOF as well as cells

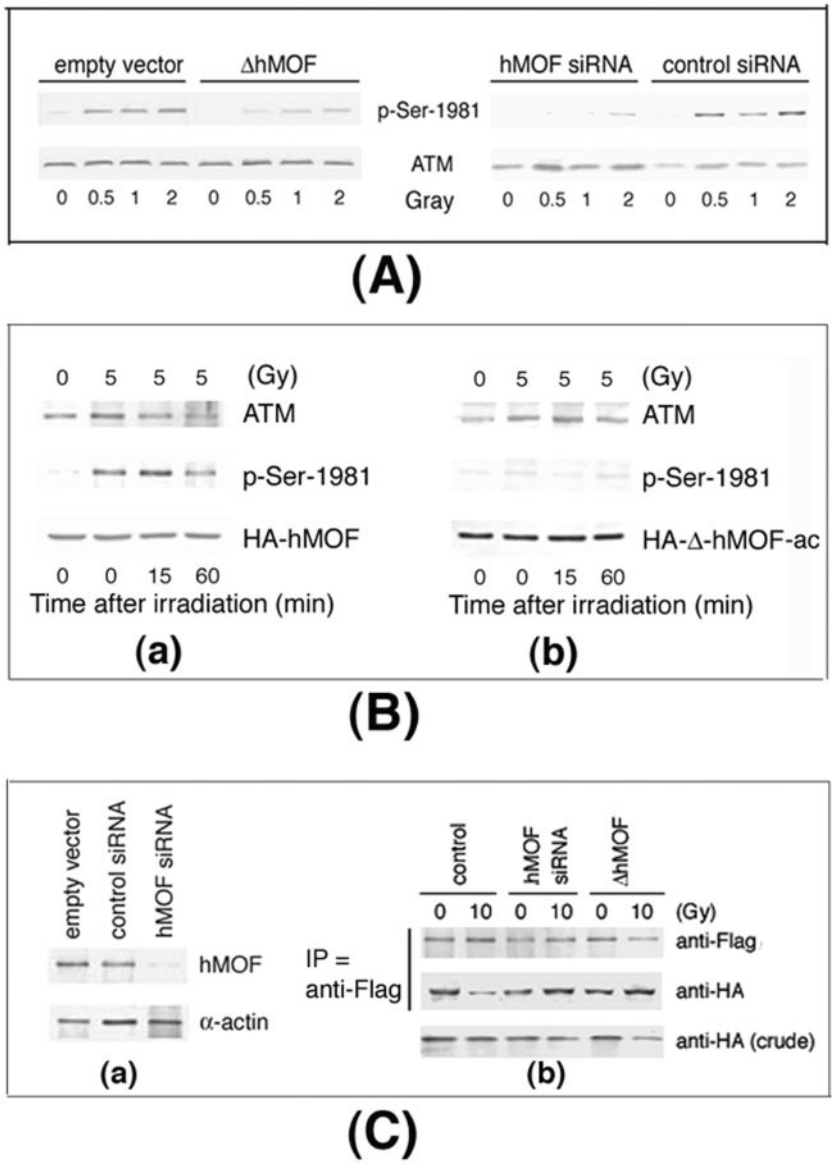

FIG. 6. hMOF inactivation influences ATM activation. (A) The expression of ΔhMOF or hMOF knockdown by siRNA resulted in a failure of IR-induced ATM autophosphorylation in 293 cells. (B) Functional hMOF association is required for IR-induced ATM autophosphorylation. 293 cells were transfected with HA-hMOF (a) or HA-ΔhMOF (b). ATM immunoprecipitated with anti-HA and tagged to hMOF showed only IR-induced ATM autophosphorylation (subpanel a), whereas ATM complexed with ΔhMOF did show loss of IR-induced ATM autophosphorylation (subpanel b). (C) hMOF inactivation influences IR-induced ATM dimer-to-monomer formation. (a) hMOF was knocked down in 293 cells by siRNA as described above. (b) Flag-tagged ATM was coexpressed with HA-tagged ATM in cells with and without functional hMOF and treated with 10 Gy. Thirty minutes after irradiation, ATM immunoprecipitated with anti-Flag was immunoblotted with anti-HA antibody. Whole-cell extract was also immunoblotted with anti-HA. Note that the loss of hMOF or the expression of ΔhMOF abrogates IR-induced conversion of ATM dimer to monomer. (D) hMOF influences IR-induced ATM kinase activity. (a) hMOF inactivation by expression of ΔhMOF or knockdown of hMOF by siRNA in 293 cells results in decreased IR-induced ATM kinase activity. ATM kinase assay was performed as described previously (41). (b) The quantitation of the bands was performed as described previously (41). (E) IR-induced acetylation of histone H4 at K16 correlates ATM activation. (a) I, Histone H4 levels and acetylation of histone H4 at K16. II, ATM and autophosphorylated ATM levels. III, ATM and phosphorylated ser15-p53 levels. (b) The quantitation of the bands in panel E(a) was performed as described previously (41). The values shown in histograms are the means from three independent experiments.

with hMOF knockdown had reduced IR-induced phosphorylation of Chk2 at Thr-68 compared to control cells (Fig. 8). These results support the argument that hMOF function influences ATM-dependent phosphorylation of its downstream DNA damage response effectors.

hMOF influences genomic stability and IR response. Cells derived from A-T individuals exhibit genomic instability and are hypersensitive to IR and radiomimetic drugs (36, 46). A-T fibroblasts also show premature senescence. Telomere loss and chromosome end-to-end associations are frequently seen in

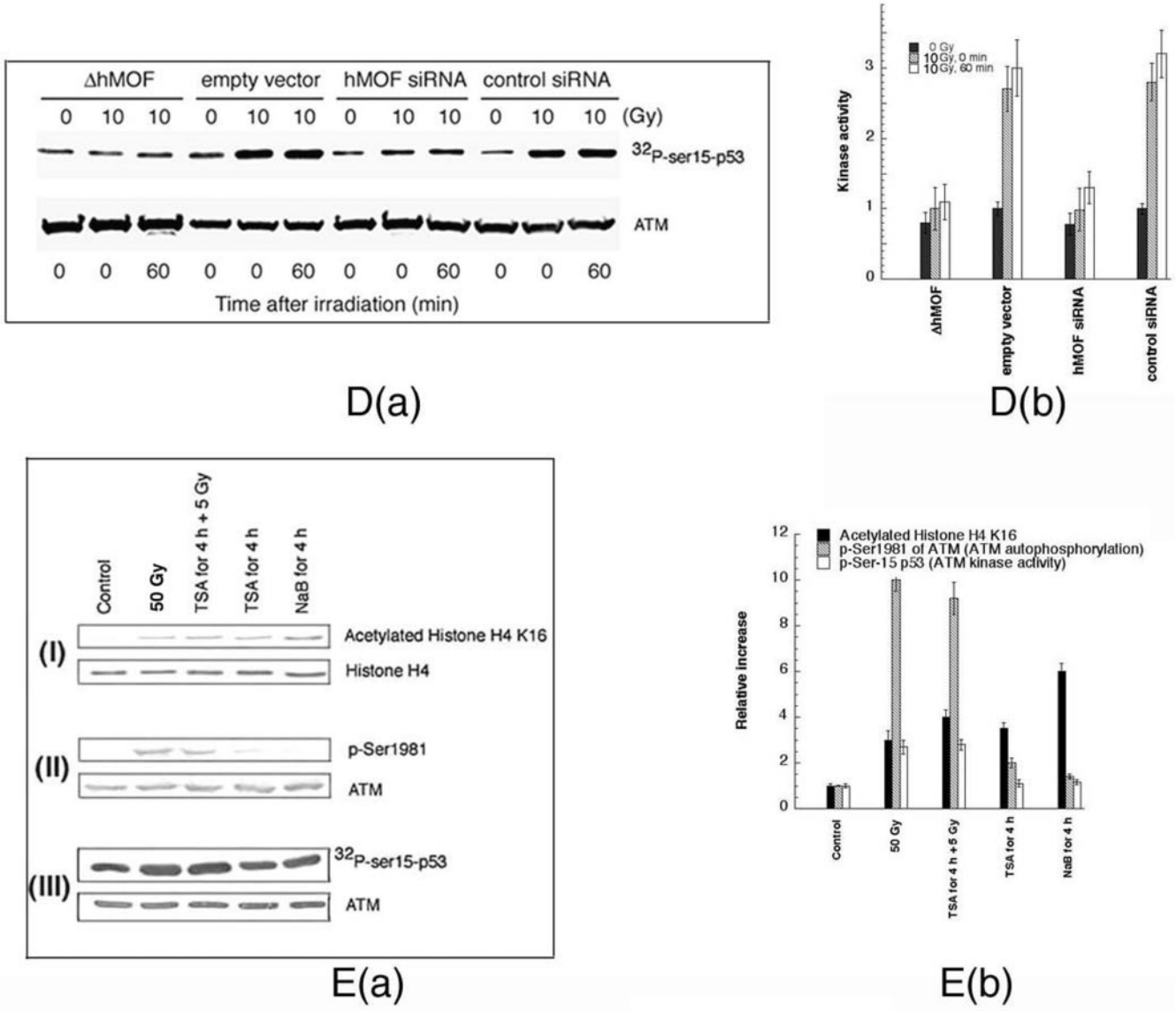

FIG. 6—*Continued*

A-T cells (36, 42). These cells exhibited approximately 0.39 chromosome end-to-end associations per metaphase, whereas the parental cells displayed 0.12 chromosome end-to-end associations per metaphase (Table 1). The increase in chromosome end-to-end association seen in cells expressing ΔhMOF is similar to that in cells with hMOF knockdown. In contrast, the overexpression of hMOF had no effect on the frequency of chromosome end associations. Since chromosome end-to-end associations may lead to anaphase bridge formation, the same cells were analyzed for anaphase bridges. Cells expressing the ΔhMOF and cells with hMOF knockdown displayed about threefold higher frequencies of anaphase bridges compared to parental cells (Table 1). Chromosome end associations and bridges can induce spontaneous chromosome as well as chromatid breaks. Cells expressing ΔhMOF and cells with hMOF knockdown displayed higher frequencies of chromatid as well as chromosome breaks when compared to parental cells (Table 1). Once again, no significant change in chromosomal break frequencies was observed in cells overexpressing wild-type hMOF (Table 1).

Consistent with the differences in spontaneous genomic damage, $ATM^{+/+}$ cells expressing ΔhMOF and cells with hMOF knockdown exhibited modest enhancements of cell killing in response to IR exposure compared to parental cells, while $ATM^{-/-}$ cells expressing ΔhMOF did not (Fig. 9). However, cells overexpressing hMOF exhibited decreased IR sensitivity for cell killing (Fig. 9). Thus, cells expressing ΔhMOF and cells with hMOF knockdown display karyotypic instability and decreased cell survival after IR exposure. All of these cellular phenotypes could be linked with defective chromosomal repair, as has been reported for cells deficient for ATM (36).

One way to address whether DNA repair is affected by hMOF function is to compare cell cycle stage-specific chromo-

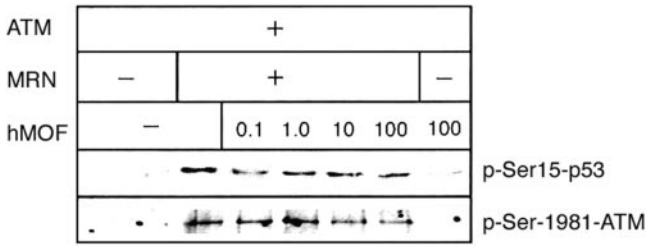

FIG. 7. hMOF is not required for ATM phosphorylation of p53 on Ser-15 by MRN in vitro. A kinase assay was performed as described previously (29). The concentration of ATM was 0.125 nM, with (+) or without (−) MRN (7.5 nM) and various concentrations of hMOF. The human ATM was expressed in human 293T cells by the transient transfection of plasmids containing full-length Flag-tagged ATM in pcDNA3. The recombinant ATM was purified on resin conjugated to anti-Flag antibodies and washed extensively with high-salt buffer before elution with Flag peptide. The recombinant MRN complex was expressed in Sf21 insect cells with a baculovirus system and was purified by nickel affinity, ion exchange, and gel filtration chromatography (29). Recombinant GST-hMOF was added to the kinase assay to determine whether it is required for purified ATM function in vitro. Addition of hMOF had no significant effect on the ATM-dependent phosphorylation of p53 or on ATM autophosphorylation in an in vitro assay.

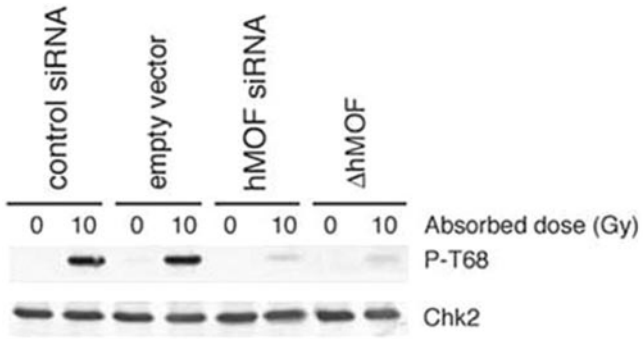

FIG. 8. hMOF inactivation influences Chk2 phosphorylation. 293 cells expressing ΔhMOF or cells with hMOF knockdown were treated with 10 Gy. Cell extracts were immunoblotted with Chk2 and Chk2 specific phospho-Threonine (P-T68) antibodies.

somal aberrations in cells with and without expression of the ΔhMOF according to the previously described procedure (45). Cells expressing ΔhMOF exhibited a significant increase in residual IR-induced G_1 chromosomal aberrations seen at metaphases (Fig. 10A). To determine whether defective repair can be documented in cells expressing ΔhMOF in phases of the cell cycle other than G_1, S-phase-specific chromosome aberrations in such cells were evaluated. Cells expressing ΔhMOF displayed higher frequencies of S-phase-specific chromatid and chromosomal aberrations per metaphase when compared to parental cells (Fig. 10B). Similar results were obtained when G_2-phase-specific chromosome aberrations were evaluated (Fig. 10C). The overexpression of hMOF resulted in a modest, although not statistically significant, decrease in residual chromosome aberrations in all the three phases of the cell cycle (Fig. 10). In addition, we used a previously described biochemical approach (38) to determine the influence of hMOF on DNA DSB repair after IR exposure. As illustrated in Fig. 11,

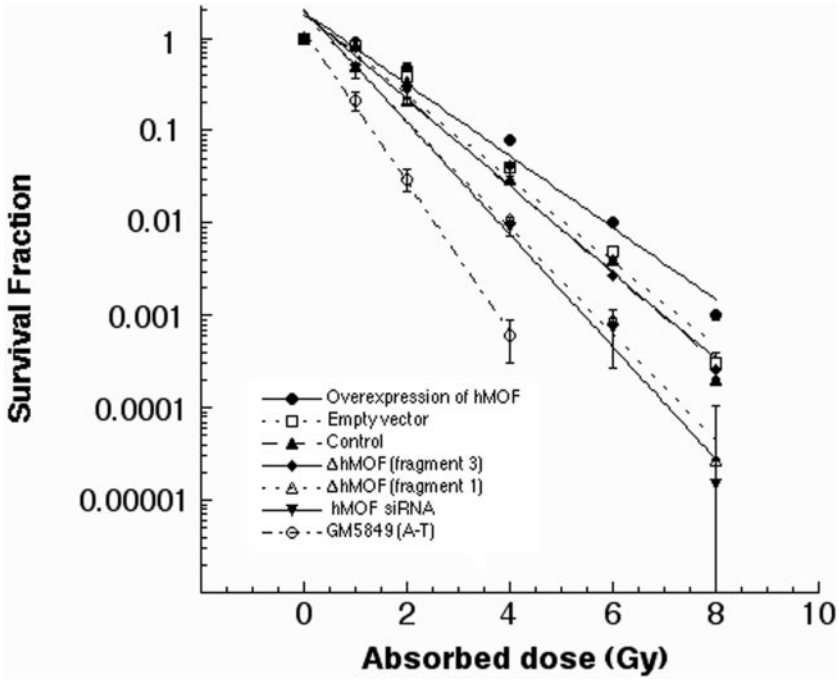

FIG. 9. hMOF influences cell survival. 293 cells expressing different fragments (fragments 1 and 3, as shown in Fig. 1A) of ΔhMOF or wild-type hMOF were exposed to different doses of ionizing radiation. Cells expressing ΔhMOF fragment 1 but not fragment 3 (shown in Fig. 1A) had reduced cell survival after IR exposure. An A-T cell line was used as a positive control. The results are the means of four experiments. The cells with expression of ΔhMOF or hMOF knockdown have statistically significant ($P < 0.01$, as determined by chi-square test) enhancements of cell killing compared to the control cells. Cells expressing wild-type hMOF have a modest reduction in cell killing compared to the control.

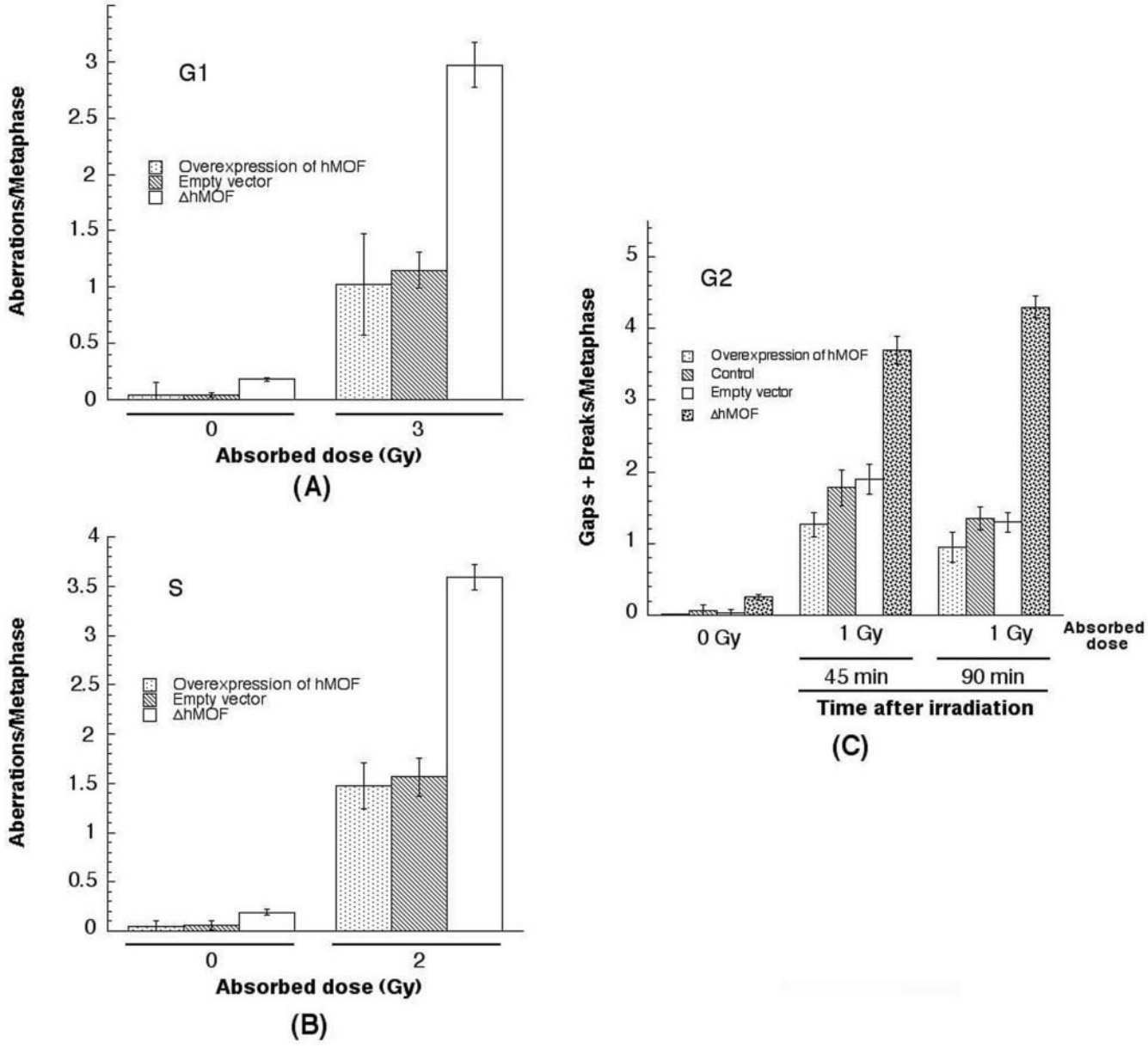

FIG. 10. Chromosome aberrations after IR treatment. (A) G_1-specific aberrations after exposure to 3 Gy. (B) S-phase-specific aberrations after irradiation with 2 Gy. (C) G_2 phase-type aberrations after irradiation with 1 Gy. The means represent the values from three independent experiments. For each experiment, 50 metaphases were scored.

TABLE 1. Spontaneous chromosomal aberrations in cells expressing mutant hMOF and cells with hMOF knockdown

Cell type	Chromosome end associations/200 metaphases	Bridges/300 anaphases	No. of[a] chromosome gaps + breaks/200 metaphases	Chromatid gaps + breaks/200 metaphases
293	24	16	2	3
293 + empty vector	21	13	3	3
293 + ΔhMOF	78*	43*	12*	7*
293 + hMOF	23	12	3	1
293 (hMOF-siRNA)	63*	51*	10*	11*
293 (control-siRNA)	19	14	4	2
HFF	12	8	2	2
GM5823 (A-T)	68*	56*	18*	12*

[a] Results in cells expressing mutant hMOF as well as in cells with hMOF knockdown are significantly different from those for controls (293 cells). Asterisks indicate that the differences are significant as assessed by chi-square analysis ($P > 0.01$).

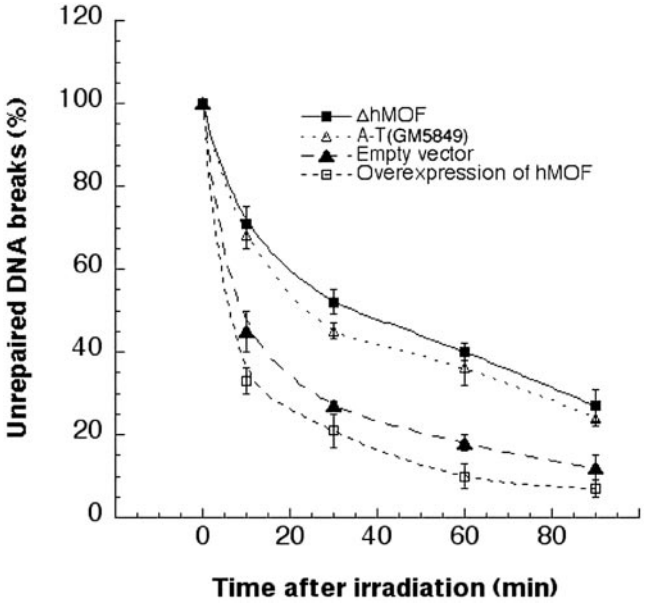

FIG. 11. DNA DSB repair analysis. Cells with and without expression of ΔhMOF or wild-type hMOF were treated with single doses of 15 Gy and lysed at different periods after irradiation according to the previously described procedure (40). A-T cells were used as a control. The unrepaired DNA breaks were measured by neutral filter elution. The data represent the means of four independent experiments.

cells expressing ΔhMOF (fragment 1 in Fig. 1A) have higher amounts of residual DNA DSBs, and cells overexpressing hMOF have relatively less residual DNA DSBs, than control cells. The observation that the expression of ΔhMOF (fragment 1 in Fig. 1A) results in a higher frequency of chromosome aberrations irrespective of which cell cycle phase was analyzed supports the idea that the inactivation of hMOF reduces the cell's capacity for global DNA repair.

A characteristic hallmark of A-T cells is the loss of the DNA-damage-induced cell cycle checkpoint (24, 36, 46). Cells expressing ΔhMOF displayed neither a significant increase in G_1 phase cells nor a decrease in S-phase entry after IR treatment compared to control cells that showed a significant decrease in S-phase entry, indicating G_1 arrest (Fig. 12A). The loss of the G_1 checkpoint seen in cells expressing ΔhMOF is similar to that in A-T cells (53), indicating that this phenotype is mimicked in cells expressing ΔhMOF. In addition to the G_1 checkpoint, IR causes a transient inhibition of DNA replication. Cells deficient in ATM function exhibit radioresistant DNA synthesis, an indicator of the loss of the S-phase checkpoint. Cells expressing ΔhMOF showed decreased inhibition of DNA synthesis, compared to the parental cells, following IR exposure (Fig. 12B). A-T cells also show defective G_2/M checkpoints after DNA damage, and ATM signaling has been shown to be required for the G_2/M checkpoint in response to IR (54). The efficiency of G_2 checkpoint control was evaluated by measuring the proportion of cells in mitosis (mitotic index) after IR exposure (11). Cells expressing ΔhMOF exhibited a decrease in mitotic index of approximately 25%, while the decrease in the parental control cells was approximately 68% (Fig. 12C). These results suggest that the inactivation of hMOF does lead to a defective G_2 checkpoint.

DISCUSSION

Members of the MYST protein family have been associated with acute myeloid leukemia (MOZ), transcriptional silencing in yeast (SAS2 and YBF2/SAS3), interactions with HIV Tat in humans (Tip60), and dosage compensation in *Drosophila* (MOF) (55). Histone acetyltransferases exist as components of multisubunit complexes involved in different processes such as transcription activation, gene silencing, and cell cycle progression as well as DNA damage repair (8). Such complexes have been reported to contain ATM-related proteins such as TRRAP, which is found in human PCAF (2). ATM is implicated in mitogenic signal transduction, chromosome condensation, meiotic recombination, cell cycle control, and telomere maintenance (36). Recently, Shahrabani-Gargir et al. (43) demonstrated that ATM controls IGF-IR gene expression in a DNA damage response pathway via a mechanism(s) involving zinc finger transcription factors Sp1 and WT1.

The interaction of hMOF with ATM is substantiated by our coimmunoprecipitation data and by the fact that we were able to map their respective regions of interaction. Using RNA interference-mediated knockdown of hMOF and a cDNA encoding an hMOF protein that lacks the C-terminal end including the acetyl-CoA binding site, we have obtained evidence that hMOF function is necessary for ATM activation. This conclusion is based on the observation that hMOF inactivation reduces IR-induced autophosphorylation of ATM as well as its kinase activity, thereby bypassing cell cycle arrest and increasing the chromosome damage. It should be noted that although the overexpression of the ΔhMOF fragment may produce nonspecific effects that would complicate the interpretation of experimental results, in the numerous experiments where both RNA interference-mediated knockdown of hMOF and ΔhMOF were used, the results obtained with these two approaches were found to be very similar.

Like its ortholog in *Drosophila*, and in contrast to all other known histone acetyltransferases, hMOF acetylates histone H4 uniquely at lysine 16. In *Drosophila*, this particular isoform of H4 is restricted to the X chromosome in males, where its presence is directly correlated to the transcriptional enhancement responsible for dosage compensation (6). In humans, it is abundantly distributed throughout the euchromatic chromosome complement (21). This observation and the extent and rapidity with which ATM is phosphorylated and monomerized following IR exposure (4) would suggest a possibility of a link between H4 acetylation by hMOF and ATM activation.

However, TSA- or NaB-induced enhancement of acetylation levels of histone H4 at K16 has minimum influence on ATM kinase activity, suggesting that modifications in the component of chromatin are not sufficient for ATM activation. Such results are consistent with the fact that ATM activation is not dependent on such chromatin modifications alone, as ATM kinase activity before and after IR exposure of S phase is similar to that of G_1- and G_2/M-phase cells (41).

A more plausible explanation for the functional interaction of hMOF and ATM is the acetylation by hMOF of ATM itself or of an unknown nonhistone protein involved in ATM activation. Acetyltransferases that acetylate both histone and nonhistone proteins include p300, CBP, PCAF, and Tip60, which acetylates the androgen receptor in addition to H2A, H3, and

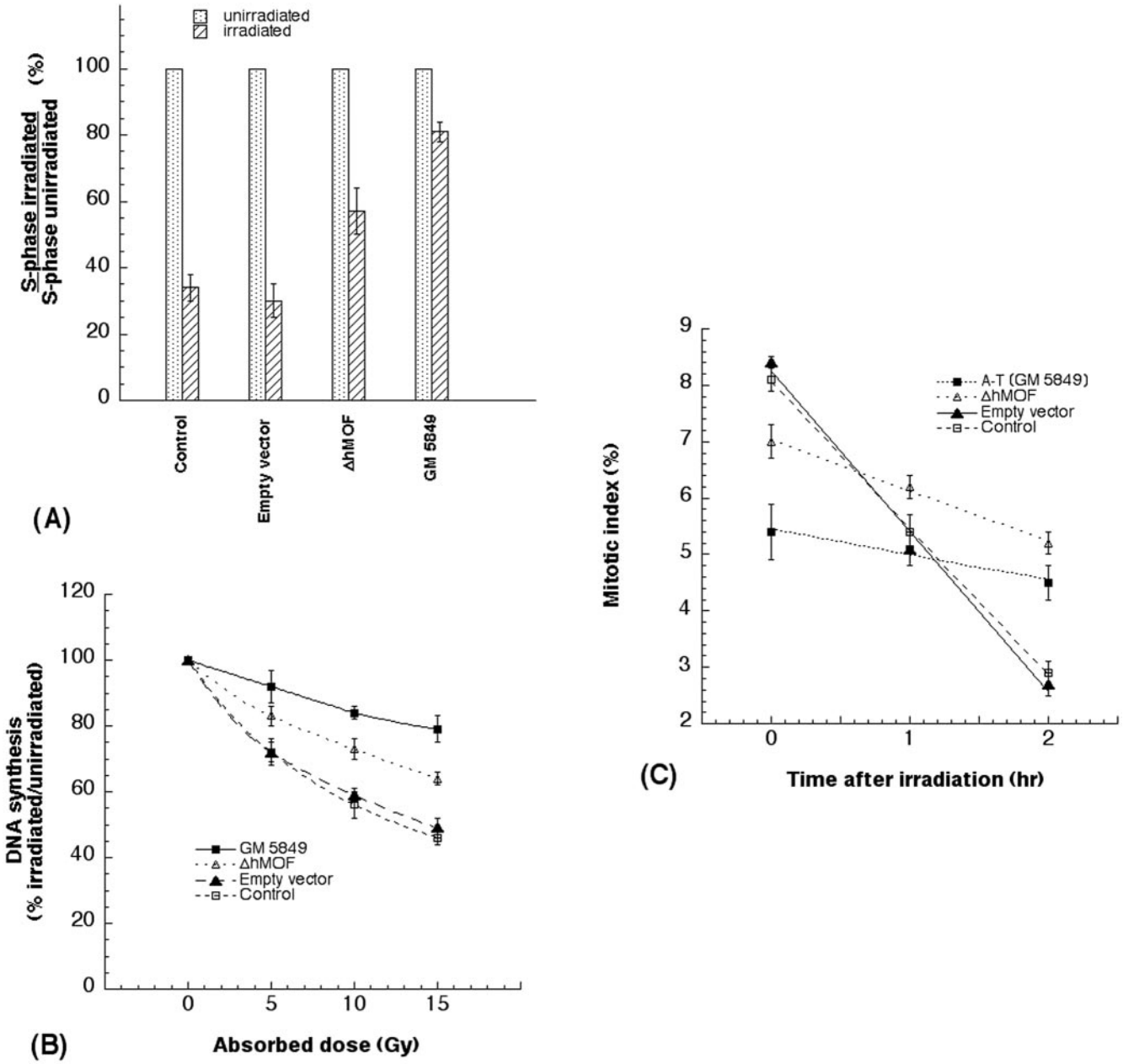

FIG. 12. Cell cycle checkpoint analysis. (A) 293 cells were irradiated with 8 Gy. Twelve hours following irradiation, cells were pulsed with bromodeoxyuridine for 30 min. The proportion of S-phase cells was determined. The percentage of S-phase cells in irradiated culture relative to that in the unirradiated control is shown. The results represent the means of three experiments. For each independent experiment, 200 cells were examined. (B) The S-phase checkpoint was determined as radioresistant DNA synthesis after exposure to ionizing radiation. 293 cells were irradiated at the doses indicated. The rate of DNA synthesis was determined 1 h postirradiation by pulse labeling with [^{3}H]thymidine for 30 min. The value of the unirradiated control was set to 100% for each cell type. The means and standard deviations of triplicate experimental points are shown. (C) Mitotic index was monitored 2 h after treatment with 2 Gy. The means represent the values from three independent experiments. For each experiment, 200 metaphases were scored.

H4 (55). More specifically, *Drosophila* MOF has been shown to acetylate MSL3 (male-specific lethal 3), another component of the dosage compensation MSL complex; the acetylation is required for specific MSL3 functions (7). Our observation that the level of H4K16-Ac is increased by exposure to IR without any apparent increase in the amount of hMOF or of its activity and irrespective of the presence of ATM can be explained by suggesting that DSBs induce a more relaxed chromatin topology, thereby increasing nucleosomal access. TSA-treated cells exhibited a very slight increase in ATM autophosphorylation without any change in ATM kinase activity in the absence of irradiation. The saturation of acetylation sites in the chromatin of these cells could free some hMOF, leading to some unscheduled acetylation of its nonhistone target(s). Whether

ATM activation could be due to the acetylation by hMOF is not known at present. Our analysis revealed that hMOF does not influence the function of monomeric ATM in an in vitro assay (Fig. 7), supporting the argument that hMOF may act as a transducer of chromatin structural alterations to ATM after DNA damage.

However, the observation that hMOF-mediated chromatin alteration in response to IR exposure correlates with ATM activation supports the proposition that chromatin structure may represent the coupling mechanism between intermolecular ATM phosphorylation and IR-induced alterations in chromatin structure, as proposed by Bakkenist and Kastan (4). Consistent with the potential role of hMOF in ATM activation is the ability of dominant negative hMOF mutations or hMOF knockdown to recapitulate the cellular characteristics of A-T cells, especially in their response to exposure to IR. hMOF plays a role in signaling the DNA damage response, as evidenced by its influence on the phosphorylation of ATM downstream effectors. Subsequent to the acetylation of histone H4 at K16 should be deacetylation in order to put back the repaired DNA into nucleosomal form. It has been elegantly demonstrated that histone H4K16 is deacetylated at sites of DSBs in yeast (20), further supporting the argument that hMOF plays a role very early in DNA damage repair. Kim et al. (27) have shown that ATM interacts with the histone deacetylase HDAC1 both in vitro and in vivo and that the extent of this association is increased after the exposure of MRC5CV1 human fibroblasts to ionizing radiation. Consistent with our results for histone H4 K16 acetylation induced by IR, Ju and Miller (22) also found no differences in H3 and H4 histone acetylation among A-T and normal cells in response to histone deacetylase inhibitor treatments.

Despite the interaction of a fraction of hMOF with ATM, hMOF-mediated acetylation of histone H4 at K16 following IR exposure is independent of ATM function. In addition, the inactivation of hMOF enhances IR-induced cell killing only in $ATM^{+/+}$ cells and not in $ATM^{-/-}$ cells, suggesting that hMOF functions upstream of ATM. The results indicating that ATM autophosphorylation occurs only in ATM associated with wild-type hMOF but not with ΔhMOF support the argument that the association of functional hMOF with ATM is critical for IR-induced ATM activation. Hasan and Hottiger (14) proposed that in DNA repair, chromosomal repression is relieved by the acetylation of histone N-terminal lysine residues, similar to the loss of chromosomal repression that allows the successful transcription of the underlying genes. Since the acetylation of the tail domain of histone H4 at K16 links with DNA repair (5) and transcription (1), further experiments are required to determine how MOF-mediated modifications discriminate the signals induced by DNA damage and transcription.

ACKNOWLEDGMENTS

We thank K. D. Brown, M. B. Kastan, S. J. Elledge, B. D. Price, and J. Chen for providing us the constructs and antibodies. We thank S. J. Elledge, S. Elgin, Y. Shiloh, S. P. Jackson, C. Hunt, N. Horikoshi, S. N. Powell, and J. Eissenberg for their comments, suggestions, and helpful discussion.

This investigation was supported by NIH (NS34746, CA10445 [project 2]), the Department of Army, the A-T Children's Society, and funds from Radiation Oncology, Washington University School of Medicine, to T.K.P. and NCI grant PO1 CA97403 (project 5) to T.L.

REFERENCES

1. **Akhtar, A., and P. B. Becker.** 2000. Activation of transcription through histone H4 acetylation by MOF, an acetyltransferase essential for dosage compensation in Drosophila. Mol. Cell **5:**367–375.
2. **Allard, S., R. T. Utley, J. Savard, A. Clarke, P. Grant, C. J. Brandl, L. Pillus, J. L. Workman, and J. Cote.** 1999. NuA4, an essential transcription adaptor/histone H4 acetyltransferase complex containing Esa1p and the ATM-related cofactor Tra1p. EMBO J. **18:**5108–5119.
3. **Allfrey, V. G., B. G. Pogo, V. C. Littau, E. L. Gershey, and A. E. Mirsky.** 1968. Histone acetylation in insect chromosomes. Science **159:**314–316.
4. **Bakkenist, C. J., and M. B. Kastan.** 2003. DNA damage activates ATM through intermolecular autophosphorylation and dimer dissociation. Nature **421:**499–506.
5. **Bird, A. W., D. Y. Yu, M. G. Pray-Grant, Q. Qiu, K. E. Harmon, P. C. Megee, P. A. Grant, M. M. Smith, and M. F. Christman.** 2002. Acetylation of histone H4 by Esa1 is required for DNA double-strand break repair. Nature **419:**411–415.
6. **Bone, J. R., J. Lavender, R. Richman, M. J. Palmer, B. M. Turner, and M. I. Kuroda.** 1994. Acetylated histone H4 on the male X chromosome is associated with dosage compensation in Drosophila. Genes Dev. **8:**96–104.
7. **Buscaino, A., T. Kocher, J. H. Kind, H. Holz, M. Taipale, K. Wagner, M. Wilm, and A. Akhtar.** 2003. MOF-regulated acetylation of MSL-3 in the Drosophila dosage compensation complex. Mol. Cell **11:**1265–1277.
8. **Carrozza, M. J., R. T. Utley, J. L. Workman, and J. Cote.** 2003. The diverse functions of histone acetyltransferase complexes. Trends Genet. **19:**321–329.
9. **Carson, C. T., R. A. Schwartz, T. H. Stracker, C. E. Lilley, D. V. Lee, and M. D. Weitzman.** 2003. The Mre11 complex is required for ATM activation and the G2/M checkpoint. EMBO J. **22:**6610–6620.
10. **Chen, S., P. Paul, and B. D. Price.** 2003. ATM's leucine-rich domain and adjacent sequences are essential for ATM to regulate the DNA damage response. Oncogene **22:**6332–6339.
11. **Dhar, S., J. A. Squire, M. P. Hande, R. J. Wellinger, and T. K. Pandita.** 2000. Inactivation of 14-3-3σ influences telomere behavior and ionizing radiation-induced chromosomal instability. Mol. Cell. Biol. **20:**7764–7772.
12. **Durfee, T., K. Becherer, P. L. Chen, S. H. Yeh, Y. Yang, A. E. Kilburn, W. H. Lee, and S. J. Elledge.** 1993. The retinoblastoma protein associates with the protein phosphatase type 1 catalytic subunit. Genes Dev. **7:**555–569.
13. **Elledge, S. J.** 1996. Cell cycle checkpoints: preventing an identity crisis. Science **274:**1664–1672.
14. **Hasan, S., and M. O. Hottiger.** 2002. Histone acetyl transferases: a role in DNA repair and DNA replication. J. Mol. Med. **80:**463–474.
15. **Hilfiker, A., D. Hilfiker-Kleiner, A. Pannuti, and J. C. Lucchesi.** 1997. mof, a putative acetyl transferase gene related to the Tip60 and MOZ human genes and to the SAS genes of yeast, is required for dosage compensation in Drosophila. EMBO J. **16:**2054–2060.
16. **Hittelman, W. N., and T. K. Pandita.** 1994. Possible role of chromatin alteration in the radiosensitivity of ataxia-telangiectasia. Int. J. Radiat. Biol. **66:**S109–S113.
17. **Horejsi, Z., J. Falck, C. J. Bakkenist, M. B. Kastan, J. Lukas, and J. Bartek.** 2004. Distinct functional domains of Nbs1 modulate the timing and magnitude of ATM activation after low doses of ionizing radiation. Oncogene **23:**3122–3127.
18. **Hwang, K. K., and H. J. Worman.** 2002. Gene regulation by human orthologs of Drosophila heterochromatin protein 1. Biochem. Biophys. Res. Commun. **293:**1217–1222.
19. **Ikura, T., V. V. Ogryzko, M. Grigoriev, R. Groisman, J. Wang, M. Horikoshi, R. Scully, J. Qin, and Y. Nakatani.** 2000. Involvement of the TIP60 histone acetylase complex in DNA repair and apoptosis. Cell **102:**463–473.
20. **Jazayeri, A., A. D. McAinsh, and S. P. Jackson.** 2004. Saccharomyces cerevisiae Sin3p facilitates DNA double-strand break repair. Proc. Natl. Acad. Sci. USA **101:**1644–1649.
21. **Jeppesen, P., and B. M. Turner.** 1993. The inactive X chromosome in female mammals is distinguished by a lack of histone H4 acetylation, a cytogenetic marker for gene expression. Cell **74:**281–289.
22. **Ju, R., and M. T. Muller.** 2003. Histone deacetylase inhibitors activate p21(WAF1) expression via ATM. Cancer Res. **63:**2891–2897.
23. **Karlseder, J., K. Hoke, O. K. Mirzoeva, C. Bakkenist, M. B. Kastan, J. H. Petrini, and T. de Lange.** 2004. The telomeric protein TRF2 binds the ATM kinase and can inhibit the ATM-dependent DNA damage response. PLoS Biol. **2:**E240. [Online.]
24. **Khanna, K. K.** 2000. Cancer risk and the ATM gene: a continuing debate. J. Natl. Cancer Inst. **92:**795–802.
25. **Khanna, K. K., and S. P. Jackson.** 2001. DNA double-strand breaks: signaling, repair and the cancer connection. Nat. Genet. **27:**247–254.
26. **Khanna, K. K., K. E. Keating, S. Kozlov, S. Scott, M. Gatei, K. Hobson, Y. Taya, B. Gabrielli, D. Chan, S. P. Lees-Miller, and M. F. Lavin.** 1998. ATM associates with and phosphorylates p53: mapping the region of interaction. Nat. Genet. **20:**398–400.
27. **Kim, G. D., Y. H. Choi, A. Dimtchev, S. J. Jeong, A. Dritschilo, and M. Jung.** 1999. Sensing of ionizing radiation-induced DNA damage by ATM through interaction with histone deacetylase. J. Biol. Chem. **274:**31127–31130.

28. **Kusch, T., L. Florens, W. H. Macdonald, S. K. Swanson, R. L. Glaser, J. R. Yates III, S. M. Abmayr, M. P. Washburn, and J. L. Workman.** 2004. Acetylation by Tip60 is required for selective histone variant exchange at DNA lesions. Science **306:**2084–2087.
29. **Lee, J. H., and T. T. Paull.** 2004. Direct activation of the ATM protein kinase by the Mre11/Rad50/Nbs1 complex. Science **304:**93–96.
30. **Lim, D. S., D. G. Kirsch, C. E. Canman, J. H. Ahn, Y. Ziv, L. S. Newman, R. B. Darnell, Y. Shiloh, and M. B. Kastan.** 1998. ATM binds to beta-adaptin in cytoplasmic vesicles. Proc. Natl. Acad. Sci. USA **95:**10146–10151.
31. **Matsuoka, S., G. Rotman, A. Ogawa, Y. Shiloh, K. Tamai, and S. J. Elledge.** 2000. Ataxia telangiectasia-mutated phosphorylates Chk2 in vivo and in vitro. Proc. Natl. Acad. Sci. USA **97:**10389–10394.
32. **McGowan, C. H.** 2002. CHK2: a tumor suppressor or not? Cell Cycle **1:**401–403.
33. **Morgan, S. E., C. Lovly, T. K. Pandita, Y. Shiloh, and M. B. Kastan.** 1997. Fragments of ATM which have dominant-negative or complementing activity. Mol. Cell. Biol. **17:**2020–2029.
34. **Neal, K. C., A. Pannuti, E. R. Smith, and J. C. Lucchesi.** 2000. A new human member of the MYST family of histone acetyl transferases with high sequence similarity to Drosophila MOF. Biochim. Biophys. Acta **1490:**170–174.
35. **Pandita, T. K.** 1983. Effect of temperature variation on sister chromatid exchange frequency in cultured human lymphocytes. Hum. Genet. **63:**189–190.
36. **Pandita, T. K.** 2003. A multifaceted role for ATM in genome maintenance. Expert Rev. Mol. Med. **5:**1–21.
37. **Pandita, T. K., and C. R. Geard.** 1996. Chromosome aberrations in human fibroblasts induced by monoenergetic neutrons. I. Relative biological effectiveness. Radiat. Res. **145:**730–739.
38. **Pandita, T. K., and W. N. Hittelman.** 1992. The contribution of DNA and chromosome repair deficiencies to the radiosensitivity of ataxia-telangiectasia. Radiat. Res. **131:**214–223.
39. **Pandita, T. K., and W. N. Hittelman.** 1995. Evidence of a chromatin basis for increased mutagen sensitivity associated with multiple primary malignancies of the head and neck. Int. J. Cancer **61:**738–743.
40. **Pandita, T. K., and W. N. Hittelman.** 1992. Initial chromosome damage but not DNA damage is greater in ataxia telangiectasia cells. Radiat. Res. **130:**94–103.
41. **Pandita, T. K., H. B. Lieberman, D. S. Lim, S. Dhar, W. Zheng, Y. Taya, and M. B. Kastan.** 2000. Ionizing radiation activates the ATM kinase throughout the cell cycle. Oncogene **19:**1386–1391.
42. **Pandita, T. K., S. Pathak, and C. R. Geard.** 1995. Chromosome end associations, telomeres and telomerase activity in ataxia telangiectasia cells. Cytogenet. Cell Genet. **71:**86–93.
43. **Shahrabani-Gargir, L., T. K. Pandita, and H. Werner.** 2004. Ataxia-telangiectasia mutated gene controls insulin-like growth factor I receptor gene expression in a deoxyribonucleic acid damage response pathway via mechanisms involving zinc-finger transcription factors Sp1 and WT1. Endocrinology **145:**5679–5687.
44. **Sharma, G. G., A. Gupta, H. Wang, H. Scherthan, S. Dhar, V. Gandhi, G. Iliakis, J. W. Shay, C. S. Young, and T. K. Pandita.** 2003. hTERT associates with human telomeres and enhances genomic stability and DNA repair. Oncogene **22:**131–146.
45. **Sharma, G. G., K. K. Hwang, R. K. Pandita, A. Gupta, S. Dhar, J. Parenteau, M. Agarwal, H. J. Worman, R. J. Wellinger, and T. K. Pandita.** 2003. Human heterochromatin protein 1 isoforms $HP1^{Hs\alpha}$ and $HP1^{Hs\beta}$ interfere with hTERT-telomere interactions and correlate with changes in cell growth and response to ionizing radiation. Mol. Cell. Biol. **23:**8363–8376.
46. **Shiloh, Y.** 2003. ATM and related protein kinases: safeguarding genome integrity. Nat. Rev. Cancer **3:**155–168.
47. **Smilenov, L. B., S. Dhar, and T. K. Pandita.** 1999. Altered telomere nuclear matrix interactions and nucleosomal periodicity in ataxia telangiectasia cells before and after ionizing radiation treatment. Mol. Cell. Biol. **19:**6963–6971.
48. **Smilenov, L. B., W. Mellado, P. H. Rao, S. G. Sawant, C. B. Umbricht, S. Sukumar, and T. K. Pandita.** 1998. Molecular cloning and chromosomal localization of Chinese hamster telomeric protein chTRF1. Its potential role in chromosomal instability. Oncogene **17:**2137–2142.
49. **Smith, E. R., A. Pannuti, W. Gu, A. Steurnagel, R. G. Cook, C. D. Allis, and J. C. Lucchesi.** 2000. The *Drosophila* MSL complex acetylates histone H4 at lysine 16, a chromatin modification linked to dosage compensation. Mol. Cell. Biol. **20:**312–318.
50. **Tse, C., T. Sera, A. P. Wolffe, and J. C. Hansen.** 1998. Disruption of higher-order folding by core histone acetylation dramatically enhances transcription of nucleosomal arrays by RNA polymerase III. Mol. Cell. Biol. **18:**4629–4638.
51. **Turner, B. M., A. J. Birley, and J. Lavender.** 1992. Histone H4 isoforms acetylated at specific lysine residues define individual chromosomes and chromatin domains in Drosophila polytene nuclei. Cell **69:**375–384.
52. **Uziel, T., Y. Lerenthal, L. Moyal, Y. Andegeko, L. Mittelman, and Y. Shiloh.** 2003. Requirement of the MRN complex for ATM activation by DNA damage. EMBO J. **22:**5612–5621.
53. **Wood, L. D., T. L. Halvorsen, S. Dhar, J. A. Baur, R. K. Pandita, W. E. Wright, M. P. Hande, G. Calaf, T. K. Hei, F. Levine, J. W. Shay, J. J. Wang, and T. K. Pandita.** 2001. Characterization of ataxia telangiectasia fibroblasts with extended life-span through telomerase expression. Oncogene **20:**278–288.
54. **Xu, B., S. T. Kim, D. S. Lim, and M. B. Kastan.** 2002. Two molecularly distinct G_2/M checkpoints are induced by ionizing irradiation. Mol. Cell. Biol. **22:**1049–1059.
55. **Yang, X. J.** 2004. The diverse superfamily of lysine acetyltransferases and their roles in leukemia and other diseases. Nucleic Acids Res. **32:**959–976.